

## Modeling, Analysis and Simulation of Voltage Sourced Converters-Based High Voltage DC Transmission System (VSC-HVDC)

Khaled M. Alawasa

Department of Electrical Engineering, Mu'tah University, Al-Karak, Jordan

e-mail: kmalawasa@mutah.edu.jo

Received: March 28, 2016

Accepted: May 7, 2016

**Abstract**— With the development in power electronics technologies and control techniques, a new generation of HVDC system has been launched based on voltage source converters (VSC-HVDC). It is a new dc transmission system technology known as "HVDC Light" and "HVDC Plus". This paper presents analysis, modeling and control of VSC-HVDC based. The operation principle and control strategies of VSC-HVDC are also explored and analyzed. Simulations for a VSC-HVDC are conducted using PSCAD/EMTDC software. The control design and system responses under several conditions such as control tracking performance, steady state and fault scenario are tested and verified. The linear frequency domain design and analysis have been verified by time-domain simulations.

**Keywords**— High voltage direct current (HVDC), Modeling, PSCAD/EMTDC, Simulation, System dynamics, Voltage sources converter (VSC).

### I. INTRODUCTION

High Voltage Direct Current (HVDC) technology is an efficient and flexible method to transmit power compared to conventional AC transmission [1], [2]. It uses power electronics technology with high power and voltage ratings. Using HVDC instead of High Voltage Alternative Current (HVAC) for high power transmission is advantageous for long power transmissions, bulk power delivery, long submarine power crossing, and low line cost and losses [3], [4]. Further, HVDC offers an economical and reliable method for asynchronous interconnections between AC networks, renewable resources integration, fast and dynamic power flow control, and power system stability improvement [5], [6].

With the development of power electronics technologies, control equipment and techniques, a new generation of HVDC has been launched based on voltage source converters (VSC-HVDC). It is a new dc transmission system technology known as "HVDC Light" [7] and "HVDC Plus" [8] by leading vendors (ABB and Siemens). VSC-HVDC converters include Insulated Gate Bipolar Transistors (IGBT'S) which are operated with high frequency Pulse Width Modulation (PWM) in order to get high speed control of both active and reactive power and to create the desired voltage waveform. As a result of using VSC technology and PWM, the VSC-HVDC has a number of potential features compared with classic HVDC (thyristor-based).

The VSC-HVDC is a mature technology; it provides several advantages over the classic HVDC such: improving system stability, connecting wind farms to an AC grid, enhancing power quality [9]-[11], lower losses, less expensive, limitation short circuit currents, grid access for weak AC networks, independent control for active and reactive power, supply of passive networks and black-start capability, high dynamic performance, low space requirements, long distance water crossing, and environmental reasons [12]-[22]. These features allows VSC-HVDC converters to be appropriate for a large range of applications related to power flow flexibility, fast response and recovery after the disturbances being

cleared. Due to these merits, VSC-HVDC has been an area of a growing interest; it is expected that VSC-HVDC will play an important role in power systems; and it will be one of the most important components of power systems in the future. Therefore, modeling, control design and simulation are important for power system studies and interactions [22]-[31]. There are many topologies for voltage source converters (VSC) available for HVDC applications such as Two-level VSCs [22] and multilevel VSCs [23], cascaded multilevel converters and modular multilevel VSC (MMC) [24]. The focus of this paper is on two levels VSC-HVDC.

A typical back to back VSC-HVDC system is presented in Fig.1. It consists of AC filters, transformers, converters, phase reactors and DC capacitors [23]-[25]. The main function of the VSC-HVDC is to transmit constant DC power from the rectifier to the inverter.

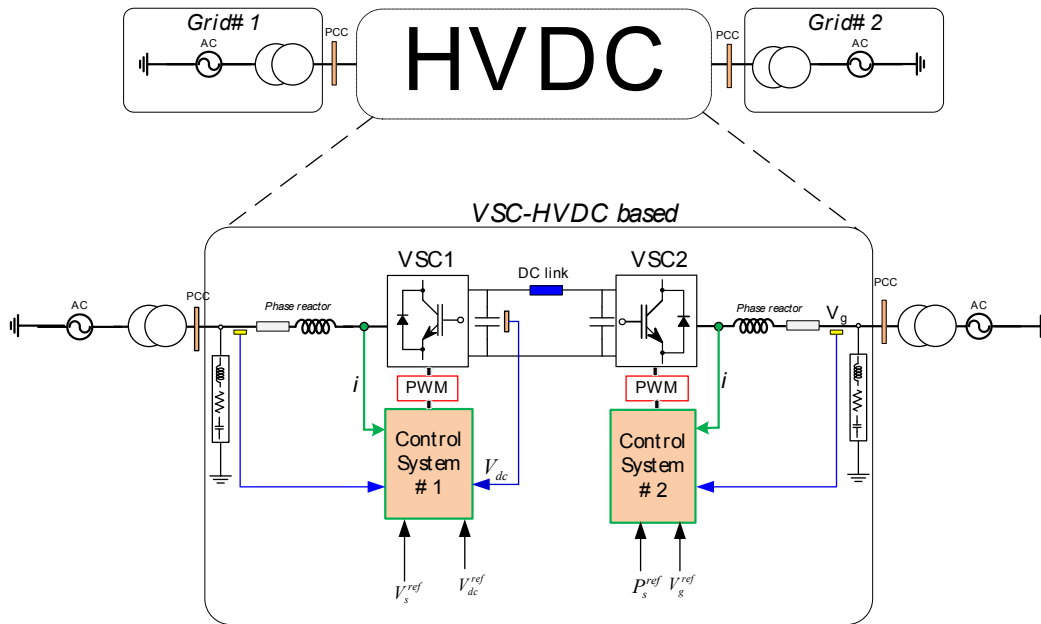


Fig. 1. Basic configuration of back to back VSC-HVDC system

## II. HVDC-VSC CONTROL STRATEGY

There is several control methods used for VSC-HVDC systems. This section provides an overview of the three control strategies [24]. Vector current control is adopted in this paper. Vector current control of VSCs was first used at variable-speed drives, where the VSC is connected to an AC motor. In this method, with respect to the point of common coupling, by controlling the phase angle and the voltage magnitude of the VSC line current, the real and reactive power can be controlled. Further, this method can independently and precisely control active and reactive power through an inner-current control loop; and it has high dynamic performance. Fig. 2 shows the main-circuit and control block diagrams of a VSC-HVDC converter using vector current control.

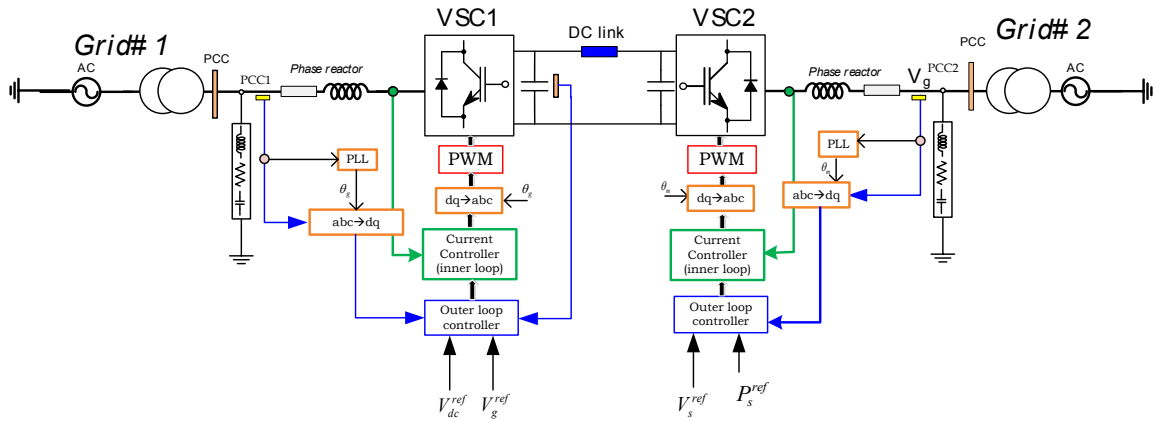


Fig. 2. Schematic diagram of VSC-HVDC system

**A. Control Design Procedure and Criteria**

In HVDC systems, the active power of the grids is transmitted only over the DC link, whereas the reactive power is exchangeable only on the AC sides and cannot be exchanged through the DC-link. Normally, the one side of HVDC system is utilized to control the DC-voltage; and the other side converter is used to regulate the active power which is typically referred to as inverter and rectifier stations, respectively. The most common control implementation is the vector control, which gives the ability to control the active and reactive powers independently. Therefore, at both sides and in parallel to the DC and active power control, the converter can be designed to 1) control the voltage at the PCC, 2) control the reactive power or to 3) maintain the unity power factor. In this paper, the control voltage at the PCC at both stations is adopted; and the control arrangement is shown in Fig. 3. It shows the control circuit for the system under the study. VSC1 is used to control the DC-voltage (DC control), while VSC2 is used to control the active power (active power control). The control is implemented in *dq*-frame; and the well known controller, PI controller, is used. Fig. 3 shows the control loop structures.

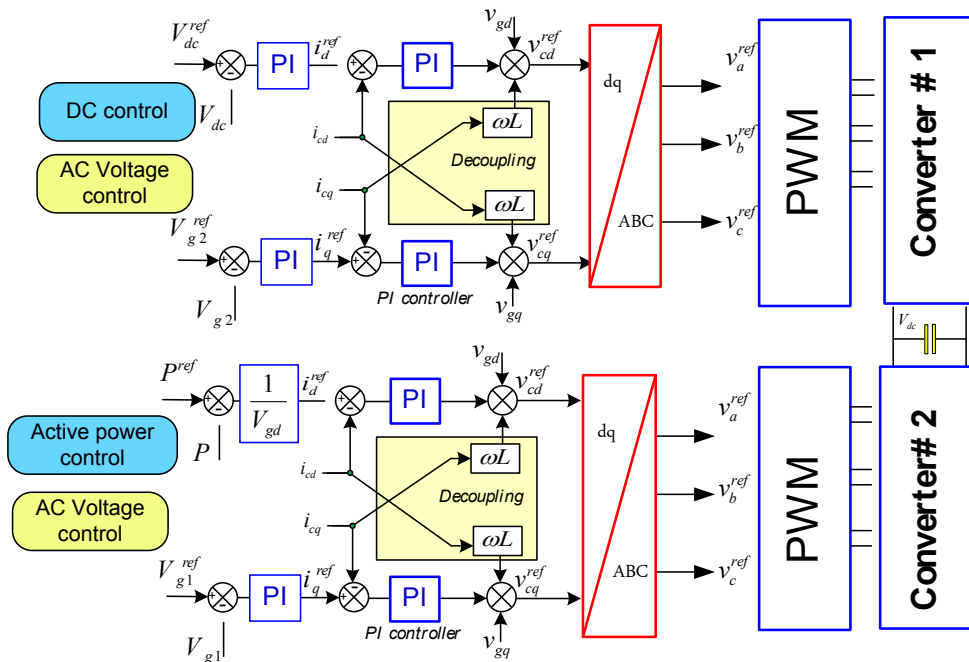


Fig. 3. Control loops and structures of VSC-HVDC system converters schematic diagram of VSC-HVDC system

### A.1. Inner Current Control Loop

Fig. 4 shows the schematic diagram of the grid-side converter. The dynamic equations in a synchronous frame rotating with the grid voltage are:

$$v_{cd} = \left( R i_d + L \frac{di_d}{dt} \right) + (v_{gd} - \omega L i_q) \quad (1)$$

$$v_{cq} = \left( R i_q + L \frac{di_q}{dt} \right) + (v_{gq} + \omega L i_d) \quad (2)$$

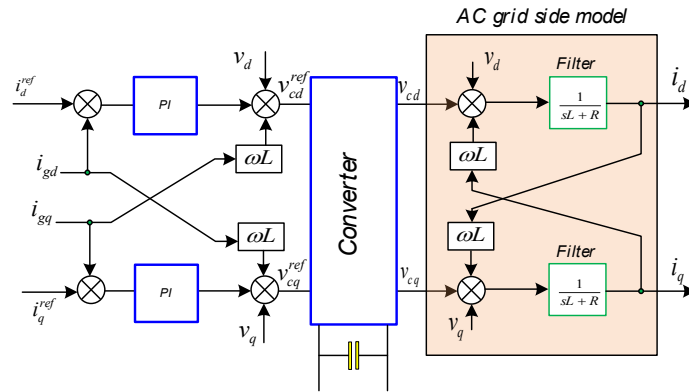


Fig. 4. Control block diagram of a current-controlled VSC-HVDC system

PI controller is the most common type in  $dq$ -frame due to its ability to track DC and low frequency signals. By combining the current system and grid side dynamic, the closed loop system is:

$$F_{cc}(s) = \frac{\left[ k_{p-cc} + \frac{k_{i-cc}}{s} \right] \left[ \frac{1}{Ls+R} \right]}{1 + \left[ k_{p-cc} + \frac{k_{i-cc}}{s} \right] \left[ \frac{1}{Ls+R} \right]} \quad (3)$$

The gains of PI controller such as  $k_{p-cc} = \frac{L}{\tau_{cc}}$  and  $k_{i-cc} = \frac{L}{\tau_{cc}}$  are selected, where  $\tau_{cc}$  is the time constant of the closed loop current controller. Equation (3) can be simplified by the first order transfer function:

$$F_{cc}(s) = \frac{1}{\tau_{cc}s+1} = \frac{\omega_{cc}}{s+\omega_{cc}}, \quad \omega_{cc} = 1/\tau \quad (4)$$

Where  $\omega_{cc}$  is the bandwidth for the closed loop current controller. The switching frequency is chosen as 1980 Hz. The recommended bandwidth for the current controller is selected as one fifth of the switching frequency [32], [33]; and the bandwidth of current controller is selected to be 15% of the switch frequency (i.e. 1866 rad/s). With  $L=0.031\text{H}$  and  $R=0.83\Omega$ , the value of PI gains are calculated ( $k_p=60$  and  $k_i=300000$ ). This designed is for both converters. Fig. 5 shows the linear frequency response of current controller closed loop systems.

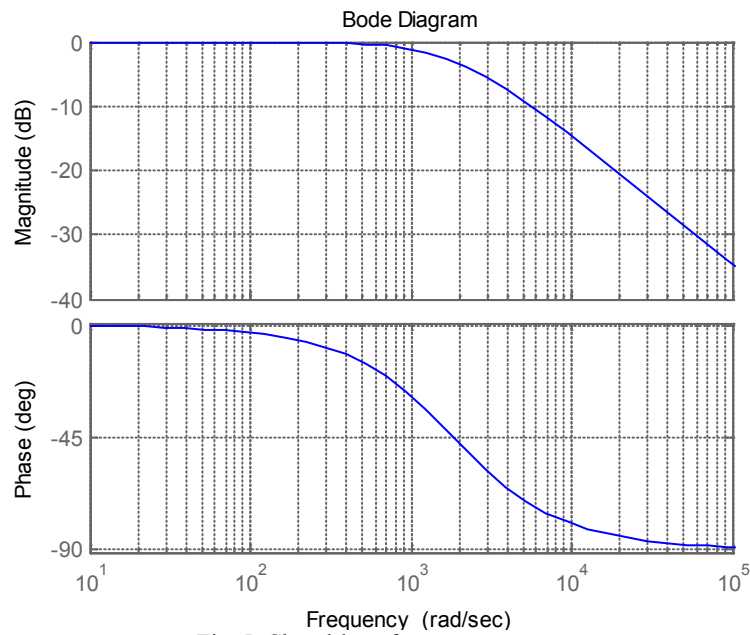


Fig. 5. Closed-loop frequency response

A.2. DC Outer Loop

In *dq*-frame control, DC control is an outer loop Fig. 6 shows the DC control structure. For a stable cascaded control operation, the recommended bandwidth for the outer controller is at least five times lower than the inner loop [34]. The bandwidth of the DC controller loop is chosen to be slower than the inner loop, with a bandwidth 10% of the inner loop, which is equal to 186 rad/s. The dynamics of the current-control loop ( $F_{cc}$ ) is much faster than the outer loops, so it is reasonable to assume that  $F_{cc} = 1$  within the bandwidth of the outer loops. The closed loops transfer function of DC control loop can be described by:

$$G_{dc} = \frac{(v_{dc}^{ref})^2}{(v_{dc})^2} = \frac{sk_{p-dc} + k_{i-dc}}{0.5s^2C + sk_{p-dc} + k_{i-dc}} \tag{5}$$

The common second-order transfer function is  $\omega_n^2 = \frac{K_{i-dc}}{0.5C}$  and  $2\zeta\omega_n = \frac{K_{p-dc}}{0.5C}$ ; where  $\zeta = 1$  and  $\omega_n = 0.67$  pu yields  $k_{p-dc} = 0.05$  and  $k_{i-dc} = 0.0454$ . Fig. 7 shows the frequency response of the DC voltage.

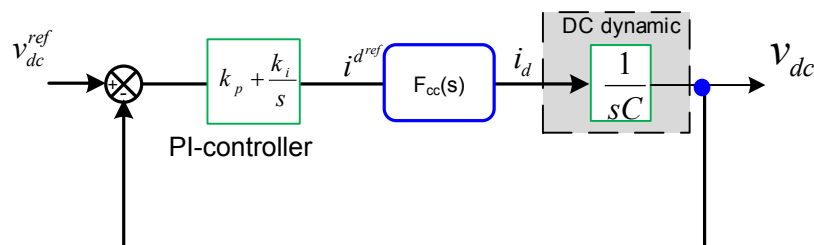


Fig. 6. Control block diagram of DC control loop

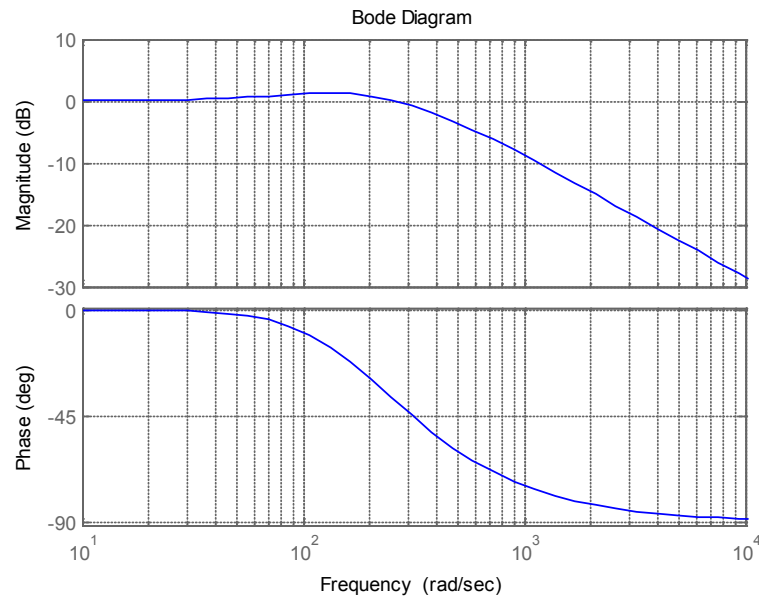


Fig. 7. Linear frequency response of DC voltage control

### A.3. Active Power Outer Loop

The power loop is a simple loop; it can be performed as shown in Fig. 8. The difference between the measured and the reference active power is used to generate the reference signal for current controller.

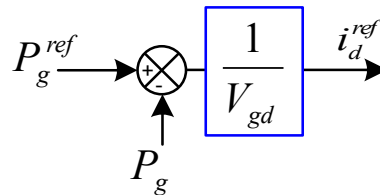


Fig. 8. Active power controller

## III. SIMULATIONS AND RESULTS

### A. Control Performance–Controller Tracking Capability

Fig. 9 shows PSCAD/EMTDC [35] block diagram implementation of the studied HVDC-VSC system.

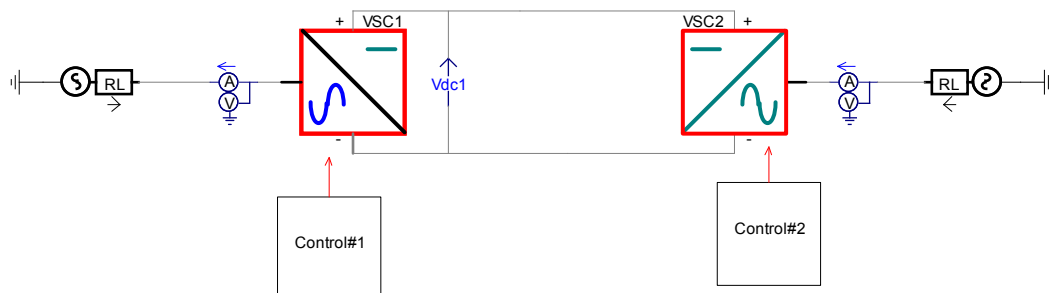


Fig. 9. PSCAD implementation for the HVDC-VSC system

Figs. 10 and 11 show control performance, control tracking capability, and response under a change in the reference signals (10% change in DC link voltage). This step is necessary for initial validation of control design. As it is presented in Fig. 10, the DC-voltage has a good tracking for its reference. Also, it is observed that the current control is much faster than the DC control which validates the linear design process. Fig. 11 shows the control response and the power at both ends. It is obvious that the controller tracks its reference in a good response. While the DC is kept constant, the sending end is able to push the power to the other end. The difference between the sending end and receiving end is the HVDC system loss.

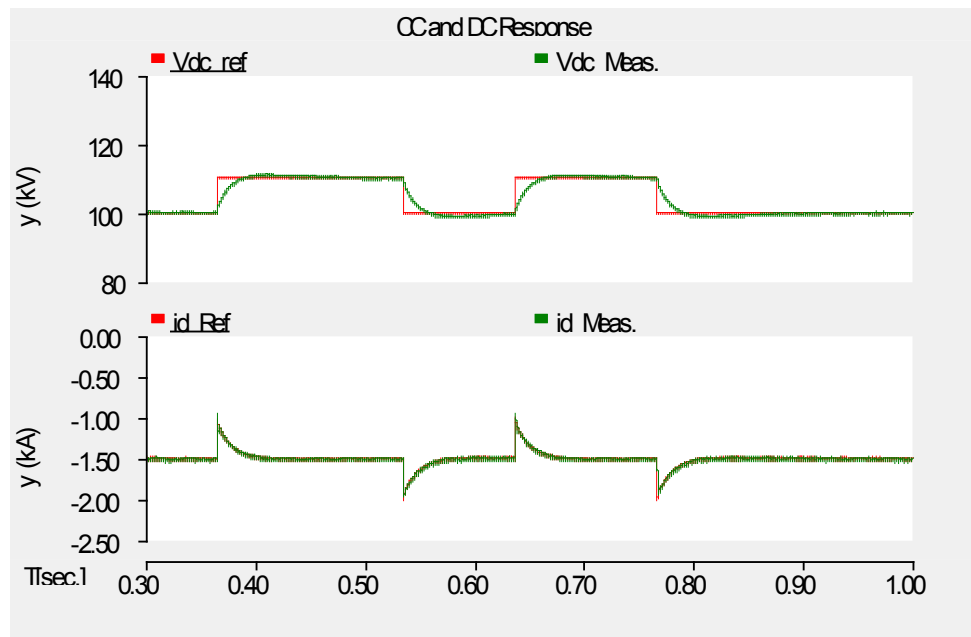


Fig. 10. DC-voltage and current control responses under 10% change in DC link voltage

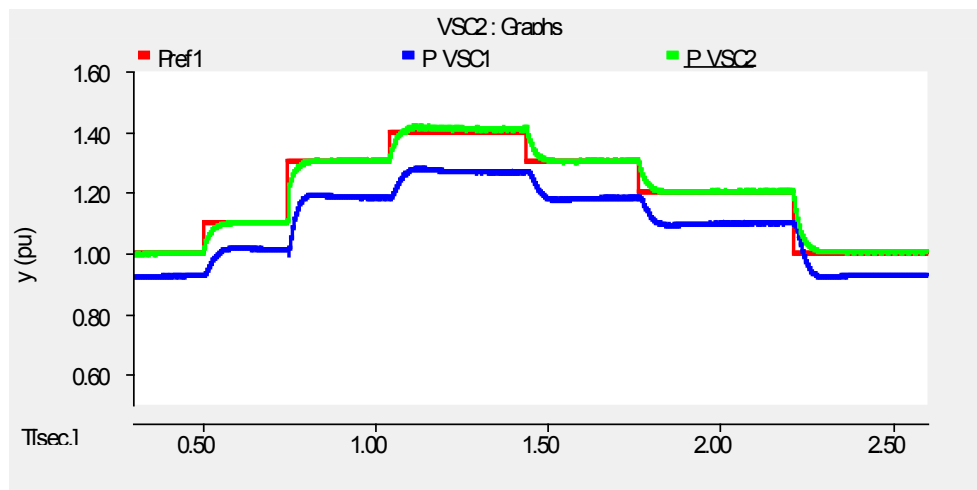


Fig. 11. Active power control response with different changes

### B. Steady State Simulation

The results shown in Figs. 12 and 13 represent the steady state condition where the case VSC2 (grid 2) is transmitting 100 MW to VSC1 (grid 1). The current, voltage waveforms for both VSC1 and VSC2, the DC-link voltage and the transmitting and receiving power are shown in both figures. The results clearly indicate that the DC-link voltage is constant and

stable; also the power received by grid1 is less than the transmitted power due to the converter losses.

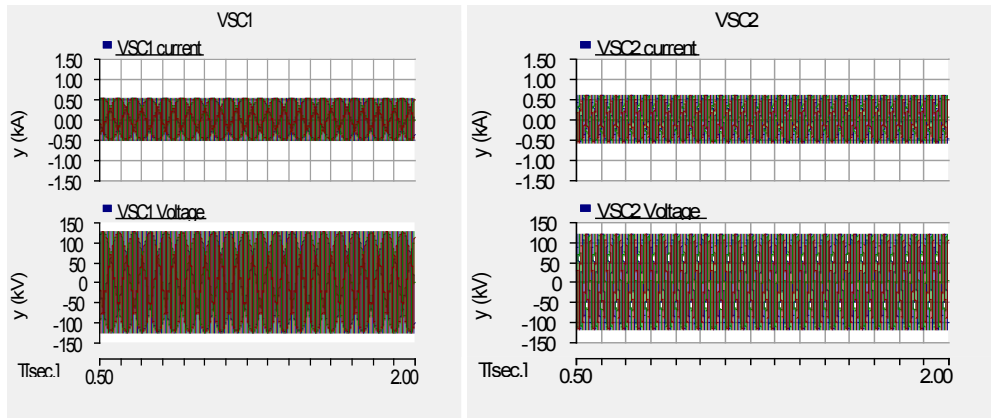


Fig. 12. Current and voltage waveforms for both VSC1 and VSC2

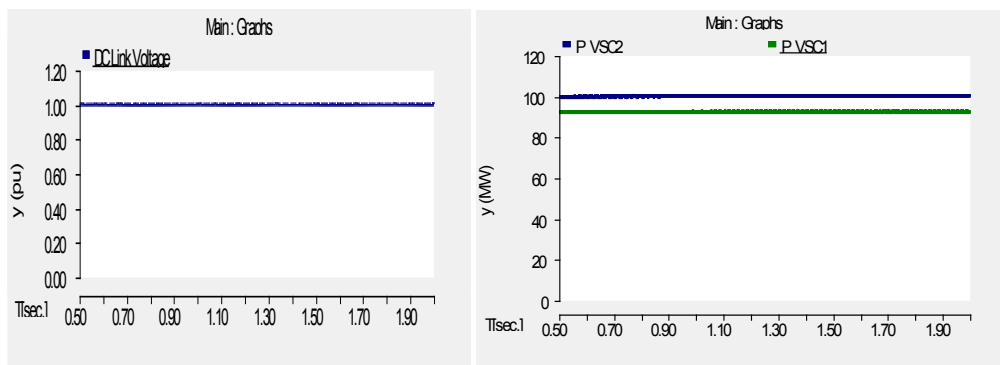


Fig. 13. System response under steady-state condition

### C. System Response under Three Phase Fault at Grid 1

Figs. 14 and 15 show the performance of HVDC under a three phase fault at grid 1. A three phase fault is applied at time  $t=1$ , for 50ms fault duration. The VSC1 current and voltage waveforms show that the system faces an over-current and voltage dip; this fault has led to increasing the DC-link voltage as the power transmitted from VSC2 is accumulated at the DC-link due to the fault at grid 1 (which made the power at the receiving end almost zero). After the fault had been cleared, the controller brought the system to the steady state condition. However, there is no impact of the fault on the other end (grid 2) since DC link acts as a buffer to isolate both ends.

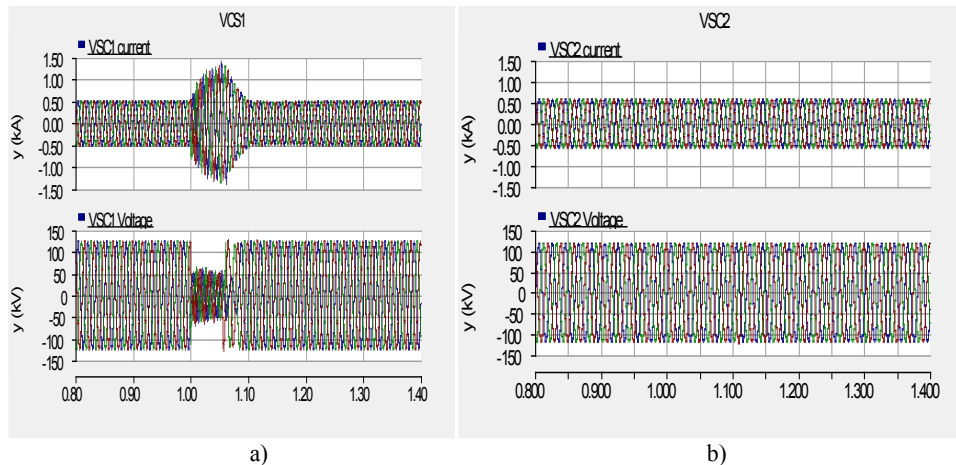


Fig. 14. System response under fault at grid 1; a) current and voltage at PCC point of grid 1, b) current and voltage at PCC point of grid 2



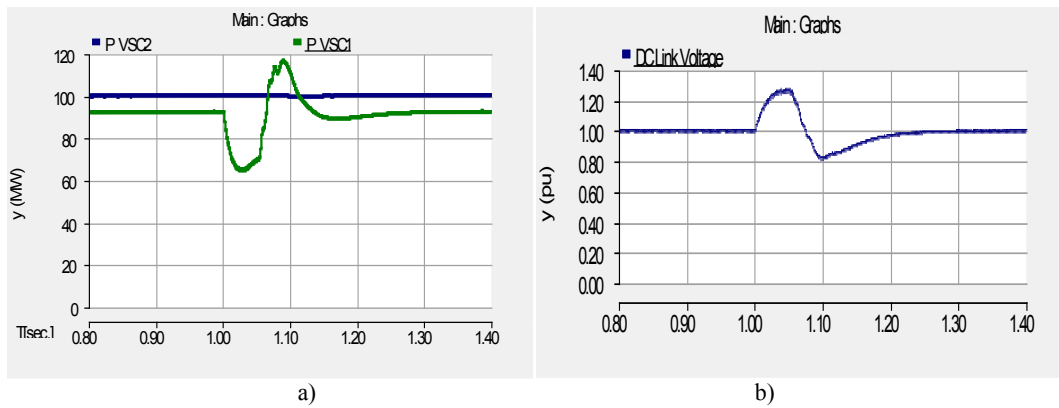


Fig. 15. System response under fault at grid 2; a) sending and receiving active Power, b) DC voltage link

**D. System Response under Three Phase Fault at Grid 2**

Figs. 16 and 17 show the system response under a three phase fault at grid 2. The VSC2 current and voltage waveforms show that the system faces an over-current and voltage dip. This fault has led to decreasing the DC-link voltage due to the fact that the power fed to the DC is reduced due to the fault. This decrease is manifested as a decrease in DC link and in the power (current) at the receiving end. In comparison, fault at grid 2, where the active power is controlled, only reduces the current. However, voltages are still not influenced in both cases.

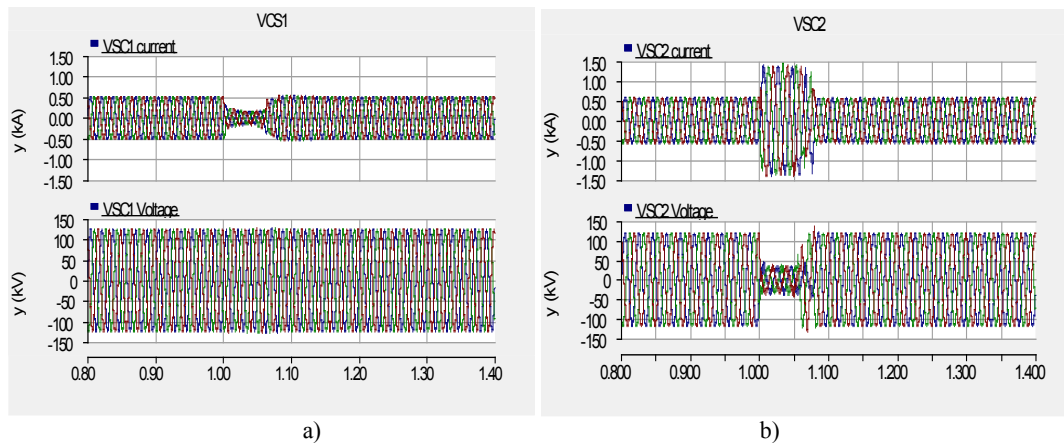


Fig. 16. System response under fault at grid 2; a) current and voltage at PCC point of grid 1, b) current and voltage at PCC point of grid 2

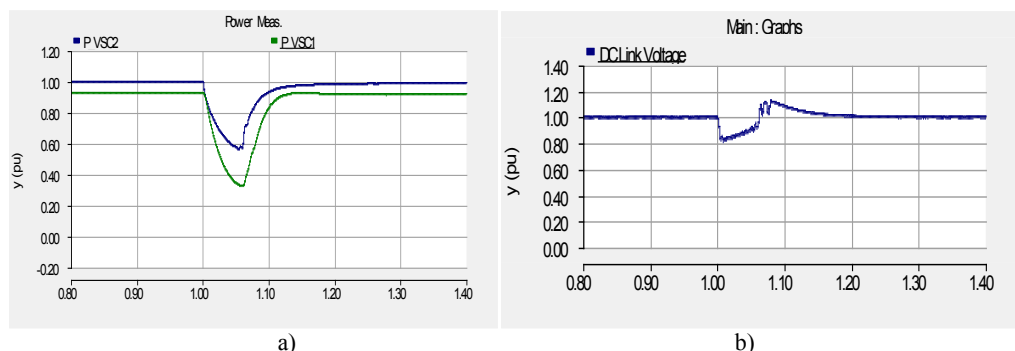


Fig. 17. System response under fault at grid 2; a) sending and receiving active power, b) DC voltage link

**E. System Response under Single Phase Fault at Grid 1**

Figs. 18 and 19 show the system response under a single phase fault (phase A) at grid 1. The VSC1 current and voltage waveforms show that the system faces an over-current and voltage

dip in phase A (faulted phase). This fault created an increase and harmonics in the DC-link voltage due to an unbalance in the voltage and current. Like three phase fault, the remote grid is not affected by this fault.

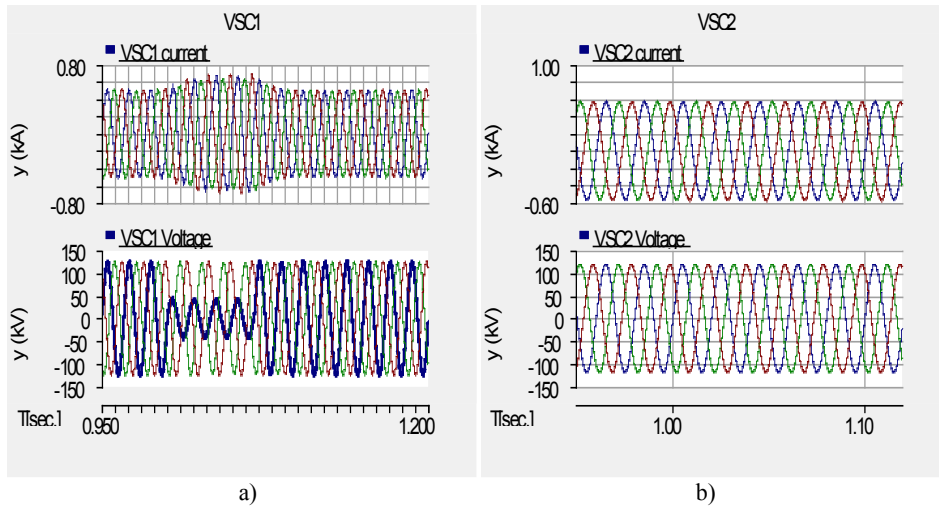


Fig. 18 System response under fault at grid2 ; (a) current and voltage at PCC point of grid 1, (b) current and voltage at PCC point of grid 2

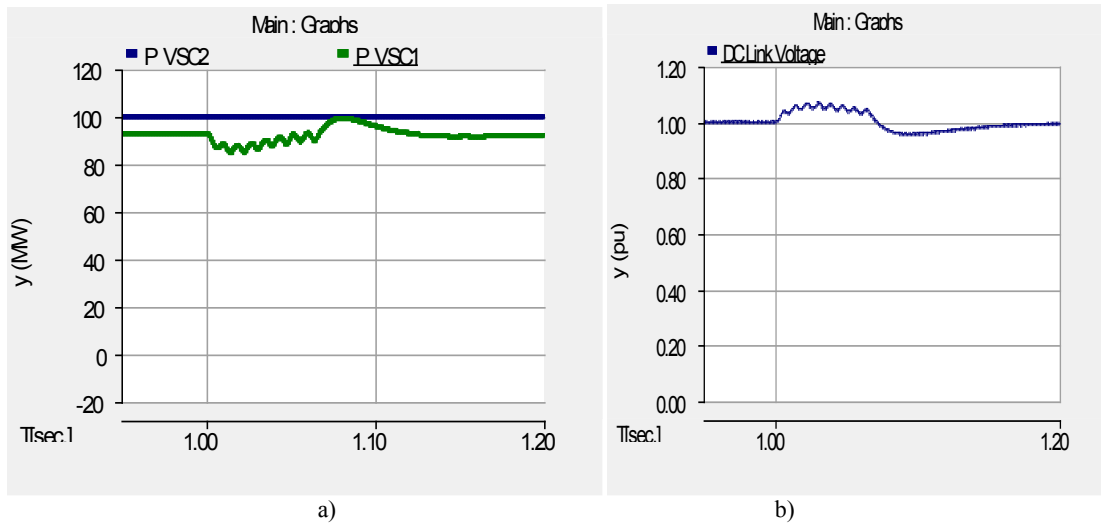


Fig. 19. System response under fault at grid 2; a) sending and receiving active power, b) DC voltage link

**F. System Response under Single Phase Fault at Grid 2**

Figs. 20 and 21 show the system response under a single phase fault (phase A) at grid 2. The VSC2 current and voltage waveforms indicate that the system faces an unbalanced over-current and voltage dip in phase A (faulted phase). This fault created a decrease and rich of harmonics in the DC-link voltage due to an unbalance in the voltage and current that is reflected on the DC link. Similarly, for the previous fault scenario, the remote grid is not influenced by this fault.

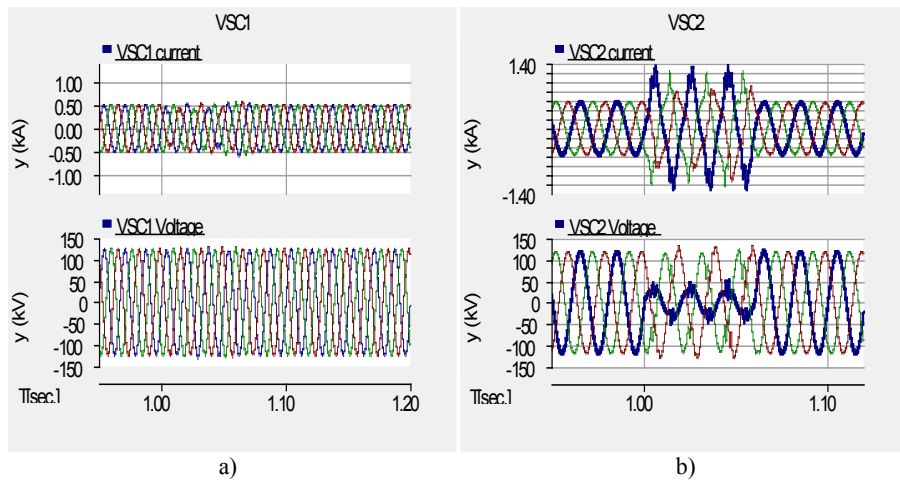


Fig. 20. System response under fault at grid 2; a) current and voltage at PCC point of grid 1, b) current and voltage at PCC point of grid 2

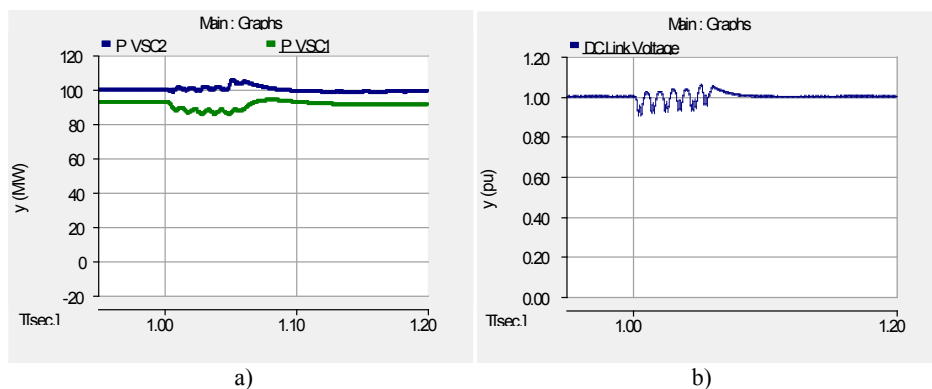


Fig. 21. System response under fault at grid 2; a) sending and receiving active power, b) DC voltage link

### G. Harmonics Analysis

Under steady state operation, the current and voltage waveforms are taken to evaluate the harmonics content of the designed VSC systems. The standard blocks in PSCAD for Fast Fourier Transform (FFT) and Total distortion harmonics (THD) block are used to determine the harmonic magnitude of the line currents and voltages. Fig. 22 shows the FFT and THD for the line current before the filter. The highest harmonic appears at harmonic order 39. These measurements are consistent with the theoretical predictions from the PWM scheme [36]. The switching frequency is 1950Hz for grid 1 and 1980Hz for grid 2 which gives frequency modulation ratio ( $m_f=39$ ). Harmonics appear as side bands, centered around the switching frequency with the highest value at  $m_f=39$ .

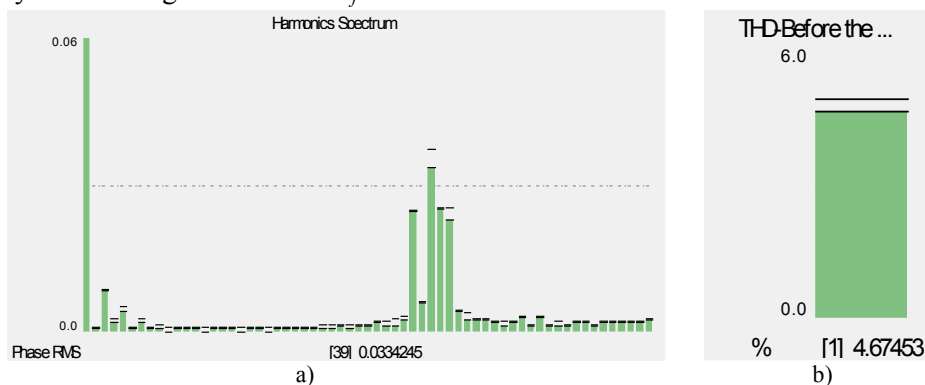


Fig. 22. Harmonics spectrum of injected current at converter terminal (before the filter), a) individual harmonic distortion (%), b) total harmonics distortion THD

Fig. 23 shows current and voltage waveforms at the point of common coupling (PCC) for grid 1. The corresponding individual harmonic, harmonic distortion and total harmonics distortion are shown in Fig. 24.

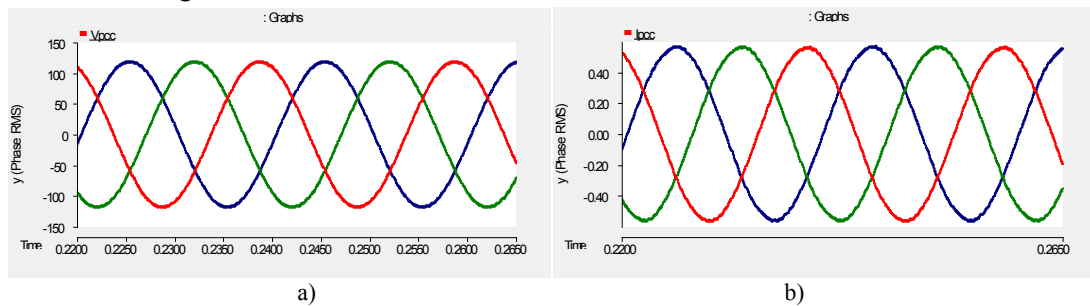


Fig. 22. Waveforms at PCC; a) voltage waveforms, b) current waveforms

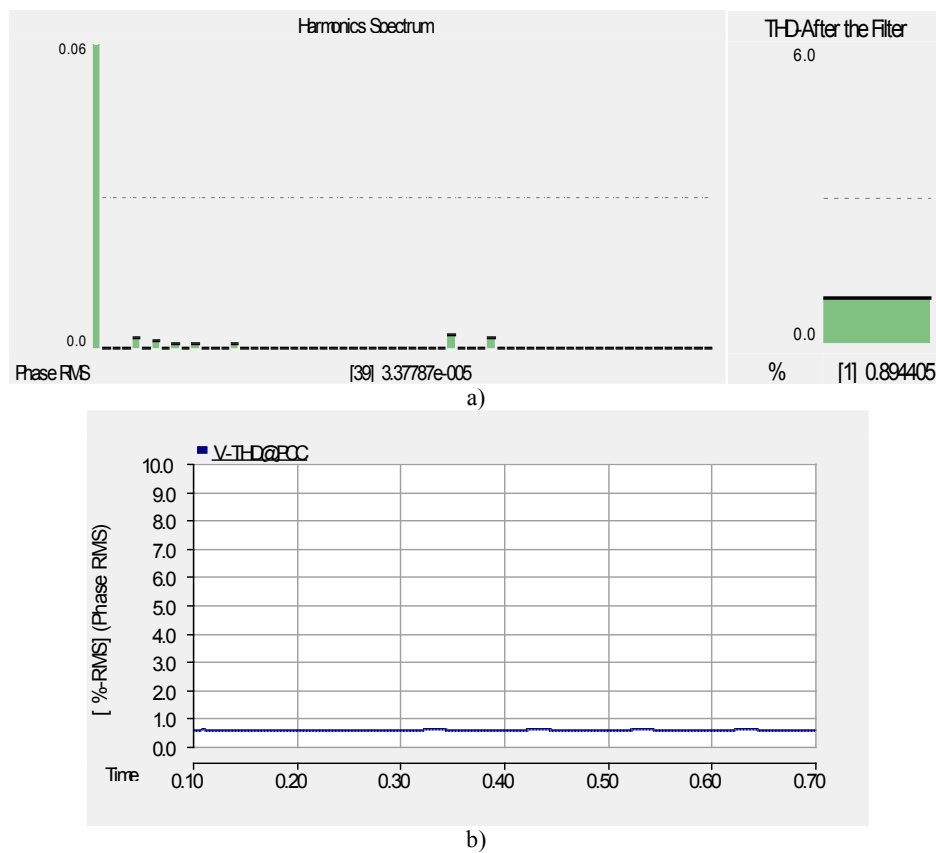


Fig. 23. Harmonics spectrum of injected current and voltage at PCC (after the filter), a) current harmonics spectrum & THD, b) voltage THD

Based on the above results, the THD levels for both of the injected current and voltage at PCC are less than 1%, which is under the maximum limit specified in IEEE standards [37].

#### IV. CONCLUSION

This paper presents analysis, modeling and control of HVDC-VSC-based. The operation principle and control strategies of VSC-HVDC are also explored and analyzed. Simulations for a back-to-back VSC-HVDC are conducted using PSCAD/EMTDC software. The simulations are conducted for connecting asynchronous grids (50 and 60Hz) as one of HVDC applications in modern power systems and grids interconnection.

Control and system response performance under both steady-state condition and grid dynamic scenario such as symmetrical and unsymmetrical fault are tested and verified. It is shown that the design controller is able to bring the system to the steady state condition after the fault is cleared. Further, the design and control responses show an excellent matching between the linear analysis (frequency domain analysis) results and those from nonlinear analysis (time domain simulation). After harmonic analysis is carried out, the converter output harmonics contents match the theoretical predictions from the PWM scheme. THD levels for both injected current and voltage at PCC are less than 1%, which is within IEEE standards limit.

## REFERENCES

- [1] N. Flourentzou, V. G. Agelidis and G. D. Demetriades, "VSC-based HVDC power transmission systems: an overview," *IEEE Transactions on Power Electronics*, vol. 24, no. 3, pp. 592-602, 2009.
- [2] V. Sood, *HVDC and Facts Controllers-Applications of Static Converters in Power Systems*. Springer Science & Business Media, 2006.
- [3] M. P. Bahrman, "Overview of HVDC transmission," *Proceedings of IEEE Power Systems Conference and Exposition*, pp. 18-23, 2006.
- [4] M. P. Bahrman, "HVDC transmission overview," *Proceedings of IEEE Transmission and Distribution Conference and Exposition*, pp. 1-7, 2008,
- [5] C. Du, *The Control of VSC-HVDC and its Use for Large Industrial Power Systems*. PhD thesis, Department of Electric Power Engineering, Chalmers University of Technology, Goteborg, Sweden, 2003.
- [6] A. Kalair, N. Abas, N. Khan, "Comparative study of HVAC and HVDC transmission systems," *Renewable and Sustainable Energy Reviews*, vol. 59, pp. 1653-1675, 2016.
- [7] [http://www.siemens.com/page/1,3771,1007570-1-12\\_0\\_0-0,00.html](http://www.siemens.com/page/1,3771,1007570-1-12_0_0-0,00.html)
- [8] F. Schettler, H. Huang and N. Christl, "HVDC transmission systems using voltage sourced converters-design and applications," *Proceedings of IEEE Summer Power Meeting*, vol. 2, pp 715-720, 2000.
- [9] CIGRE SC-B4 WG 37 "VSC transmission," Cigre SC-4, *Final Document*, 2005.
- [10] M. P. Bahrman and B. K. Johnson, "The ABCs of HVDC transmission technologies," *IEEE Power and Energy Magazine*, vol. 5, no. 2, pp. 32-44, 2007.
- [11] M. Davies, M. Dommaschk, J. Dorn, J. Lang, D. Retzmann and D. Soerangr, *HVDC PLUS-Basics and Principles of Operation*. Siemens AG-Energy Sector, 2011
- [12] CIGRE SC-B4 WG 39 "Integration of large scale wind generation using HVDC and power electronics," Cigre SC-4, *Final Document*, 2009.
- [13] B. Chuco, E. H. Watanabe, "A comparative study of dynamic performance of HVDC system based on conventional VSC and MMC-VSC," *Proceedings of Bulk Power System Dynamics and Control Symposium*, pp.1-6, 2010.
- [14] G. Asplund, "Ultra high voltage transmission," *ABB Review*, vol. 2, pp. 22-27, 2007.
- [15] G. Asplund, K. Eriksson and K. Svensson, "HVDC light-DC transmission based on voltage-sourced converters," *ABB Review*, vol. 1, pp. 4-9, 1998.

- [16] G. Asplund, K. Eriksson and O. Tollerz, "HVDC light: a tool for electric power transmission to distant load," *Proceedings of VI Sepope Conference*, pp. 1-7, 1998.
- [17] B. Andersen and C. Barker, "A new era in HVDC?," *IEE Review*, vol. 46, no. 2, pp. 33-39, 2000.
- [18] G. Asplund, "Application of HVDC light to power system enhancement," *Proceedings of IEEE Power Engineering Society Winter Meeting*, pp. 2498-2503, 2000.
- [19] K. Eriksson, "Operational experience of HVDC light TM," *Proceedings of AC-DC Power Transmission International Conference*, pp. 205-210, 2001.
- [20] S. G. Johansson, L. Carlsson and G. Russberg, "Explore the power of HVDC light-a web based system interaction tutorial," *Proceedings of IEEE Power Systems Conference and Exposition*, pp. 839-842, 2004.
- [21] D. A. Woodford, *HVDC Transmission*, Manitoba Research Center, 1998.
- [22] N. Flourentzou, V. Agelidis, G. Demetriades, "VSC-based HVDC power transmission systems: an overview," *IEEE Transactions on Power Electronics*, vol. 24, no. 3, pp.592-602, 2009.
- [23] M. A. Djehaf, S. A. Zidi, Y. I. Kobibi and S. Hadjeri, "Modeling of a multi-level converter based VSC HVDC supplying a dead load," *Proceedings of Electrical and Information Technologies International Conference*, pp. 218-223, 2015.
- [24] T. Westerweller, K. Friedrich, U. Armonies, A. Orini, D. Parquet and S. Wehn, "Trans bay cable-world's first HVDC system using multilevel voltage-sourced converter," *Proceedings of CIGRE*, pp. B4-101, 2010.
- [25] C. Bajracharaya, *Control of VSC-HVDC for Wind Power*, MSc. Thesis, Norwegian University of Science and Technology, 2008.
- [26] F. Schettler, H. Huang and N. Christl, "HVDC transmission systems using voltage source convertes-design and applications," *Proceedings of IEEE Power Engineering Society Summer Meeting*, vol.2, 2000.
- [27] S. Bernet, "State of the art and developments of medium voltage converters- an overview," *Przegląd Elektrotechniczny (Electrical Review)*, vol. 82, pp. 1-10, 2006.
- [28] Siemens AG. ROBICON Perfect Harmony. [Online]. Available: <http://www.industry.siemens.com/drives/global/en/converter/mv-drives/sinamics-perfect-harmony/pages/sinamics-perfect-harmony.aspx>, accessed March 2016.
- [29] J. Pan, R. Nuqui, L. Tang and P. Holmberg, "VSC-HVDC control and application in meshed networks," *Proceedings of IEEE PES General Meeting*, 2008.
- [30] G. Ding, G. Tang, Z. He and M. Ding, "New technologies of voltage source converter (VSC) for HVDC transmission system based on VSC," *Proceedings of IEEE Power and Energy Society General Meeting- Conversion and Delivery of Electrical Energy in the 21<sup>st</sup> Century*, pp.1-8, 2008.
- [31] M. H. Okba, M. H. Saied, M. Z. Mostafa, T. M. Abdel-Moneim, "High voltage direct current transmission- a review, part I," *IEEE Energytech*, pp.1-7, 2012.
- [32] A. Yazdani and R. Iravani, *Voltage-Sourced Converters in Power Systems*, New York: Wiley, 2009.
- [33] L. Harnefors and H. P. Nee, "Model-based current control of ac drives using the internal model control method," *IEEE Transaction on Industry Applicatoions*, vol. 34, no. 1, pp. 133-141, 1998.

- [34] K. J. Åstrom and T. Hagglund, *PID Controllers*, 2<sup>nd</sup> Edition, Instrument Society of America, 1994.
- [35] Manitoba HVDC Research Centre, *PSCAD/EMTDC User Manual*, PSCAD v.4.2.1 Manitoba, 2003.
- [36] N. Mohan, T. M. Undeland, and W. P. Robbins, *Power Electronics: Converters, Applications, and Design*, 3<sup>rd</sup> ed. Hoboken, NJ: John Wiley & Sons, 2003/2007.
- [37] IEEE Recommended Practices and Requirements for Harmonic Control in Electrical Power Systems, IEEE Std. 519, 1992.